Acta Crystallographica Section D
Biological Crystallography
ISSN 0907-4449

Structures of *Plasmodium falciparum* triosephosphate isomerase complexed to substrate analogues: observation of the catalytic loop in the open conformation in the ligand-bound state

S. Parthasarathy,[a] Hemalatha Balaram,[b] P. Balaram[a] and M. R. N. Murthy[a]*

[a]Molecular Biophysics Unit, Indian Institute of Science, Bangalore 560 012, India, and [b]Molecular Biology and Genetics Unit, Jawaharlal Nehru Center for Advanced Scientific Research, Bangalore 560 064, India

Correspondence e-mail: mrn@mbu.iisc.ernet.in

Received 26 June 2002
Accepted 15 August 2002

PDB References: PfTIM–3PG, 1m7o, r1m7osf; PfTIM–G3P, 1m7p, r1m7psf.

The glycolytic enzymes of *Plasmodium falciparum* (Pf) are attractive drug targets as the parasites lack a functional tricarboxylic cycle and hence depend heavily on glycolysis for their energy requirements. Structural comparisons between Pf triosephosphate isomerase (PfTIM) and its human homologue have highlighted the important differences between the host and parasite enzymes [Velanker *et al.* (1997), *Structure*, **5**, 751–761]. Structures of various PfTIM–ligand complexes have been determined in order to gain further insight into the mode of inhibitor binding to the parasite enzyme. Structures of two PfTIM–substrate analogue complexes, those of 3-phosphoglycerate (3PG) and glycerol-3-phosphate (G3P), have been determined and refined at 2.4 Å resolution. Both complexes crystallized in the monoclinic space group $P2_1$, with a molecular dimer in the asymmetric unit. The novel aspect of these structures is the adoption of the 'loop-open' conformation, with the catalytic loop (loop 6, residues 166–176) positioned away from the active site; this loop is known to move by about 7 Å towards the active site upon inhibitor binding in other TIMs. The loop-open form in the PfTIM complexes appears to be a consequence of the S96F mutation, which is specific to the enzymes from malarial parasites. Structural comparison with the corresponding complexes of *Trypanosoma brucei* TIM (TrypTIM) shows that extensive steric clashes may be anticipated between Phe96 and Ile172 in the 'closed' conformation of the catalytic loop, preventing loop closure in PfTIM. Ser73 in PfTIM (Ala in all other known TIMs) appears to provide an anchoring water-mediated hydrogen bond to the ligand, compensating for the loss of a stabilizing hydrogen bond from Gly171 NH in the closed-loop liganded TIM structures.

1. Introduction

Antimalarial research has received considerable attention recently owing to the emergence of resistant strains of the malarial parasites (Olliaro & Yuthavong, 1999; Winstanley, 2000). Malaria caused by *Plasmodium falciparum* (Pf) is the most virulent, compared with that caused by other *Plasmodium* species. The glycolytic enzymes of the malarial parasite are attractive targets for the development of antimalarials since in the asexual stage of the parasite in the human erythrocytes glycolysis is the sole source to meet the energy requirement of the parasite (Roth *et al.*, 1988). As a part of a program to develop Pf triosephosphate isomerase (PfTIM) as a drug target (Subbayya *et al.*, 1997), we have determined structures of unliganded (Velanker *et al.*, 1997) and liganded forms of the enzyme.

TIM catalyses the isomerization between dihyroxyacetone phosphate (DHAP) and D-glyceraldehyde-3-phosphate (D-GAP). The active site of the enzyme is essentially composed of the triad Lys12, His95 and Glu165 (Alber *et al.*, 1987). Apart from these residues, an 11-residue loop, known as the flexible or catalytic loop (loop 6, residues 166–176), plays a crucial role in preventing phosphate elimination of the *cis*-enediol intermediate leading to the production of cytotoxic methylglyoxal (Pompliano *et al.*, 1990; Knowles, 1991). The PfTIM sequence is unique in that there is a Phe at position 96, proximal to the active site, which is Ser in enzymes from other sources (Parthasarathy *et al.*, private communication). In spite of this mutation, PfTIM is fully catalytically competent, with k_{cat} and K_m values of $2.68 \pm 0.84 \times 10^5$ min^{-1} and 0.35 ± 0.16, respectively, for glyceraldehyde-3-phosphate (GAP) as substrate (Singh *et al.*, 2001). This mutation, however, seems to greatly influence the conformation of the catalytic loop. Loop 6 of TIM has almost always been observed in the 'closed' conformation in crystal structures of ligand complexes. We have obtained both loop-open and loop-closed conformations of PfTIM in the presence of the transition-state analogue phosphoglycolate (PG; Parthasarathy *et al.*, private communication). Structural analysis of the loop-open form of the PfTIM–PG complex suggests that a possible steric clash between the bulky Phe96 residue and Ile170 (a flexible loop residue) hinders the loop closure. However, in the structure of the loop-closed form of the PfTIM–PG complex, residues Phe96 and Leu167 occur in alternative conformations, both of which are different from those observed in the unbound and ligand-bound loop-open forms of PfTIM. Except for this complex and that of trypanosomal TIM with 4-hydroxyphosphonobutanamide (4PBH; Verlinde *et al.*, 1992), where the bulky ligand was specifically selected to prevent the loop closure, TIM–ligand complexes have always been observed with loop-closed conformations. The observation of the ligand-bound loop-open form of PfTIM–PG complex prompted the investigation of other PfTIM inhibitor complexes with the view of assessing the relation between inhibitor structure and loop conformation in the complex. We describe in this report the structures of the complexes of PfTIM with 3-phosphoglycerate (3PG) and with glycerol-3-phosphate (G3P; Fig. 1 shows the chemical structures) at 2.4 Å resolution. The structures represents additional examples of novel loop-open conformation of PfTIM. Implications of these structures for inhibitor design are discussed.

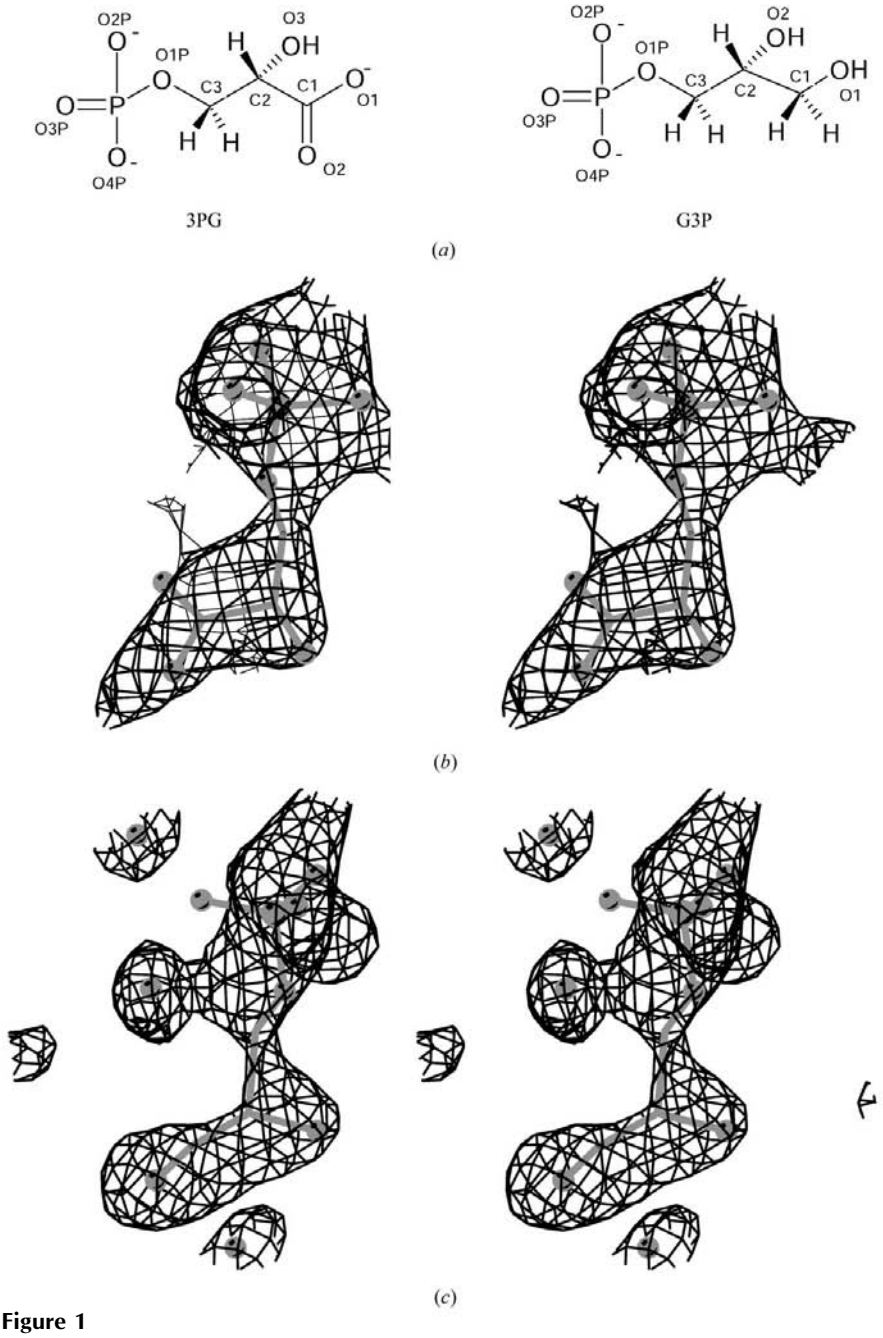

Figure 1
Chemical structures of the substrate analogues 3-phosphoglycerate (3PG) and glycerol-3-phosphate (G3P) (*a*). $mF_o - DF_c$ omit maps for the ligand 3PG (*b*) and G3P (*c*) at the end of the refinement. Maps are contoured at 2.2σ.

2. Materials and methods

2.1. Purification of PfTIM

Cloning, overexpression and purification of PfTIM followed previously established procedures (Velanker *et al.*, 1997; Ranie *et al.*, 1993). Briefly, the gene for

PfTIM was cloned into pTrc 99A vector, known as pARC 1008, and overexpressed in *Escherichia coli* strain AA200, which has a null mutation in the host TIM gene. The cells were initially grown in 100 ml of Luria broth for about 6 h at 310 K and transferred to 1 l of Terrific broth. After 4 h, cells were induced using IPTG and growth was continued for a further 8 h. Cells were harvested (centrifuged at 5000 rev min^{-1} for 20 min at 277 K), washed with minimal volume of Tris buffer pH 7.4 and crushed using a French press. Proteins dissolved in the cell lysate were initially precipitated using 70% [42%(*w*/*v*)] saturated ammonium sulfate and then at 95% [63%(*w*/*v*)] saturation. The resultant ammonium sulfate pellet dissolved in about 5 ml of cold water was dialyzed extensively against 20 m*M* Tris buffer pH 8.0. Protein was further purified using an anion-exchange Resource Q (from Pharmacia) column using an FPLC system. A 0–0.5 *M* NaCl gradient was used for eluting the protein. Alternatively, pure protein could also be obtained by subjecting the dialyzed pellet to two rounds of gel filtration on a Sephadex G-100 column. The final purity of the protein was checked using both SDS–PAGE and ESI–MS. Better crystals, however, were obtained with protein samples purified using a Resource Q column.

2.2. Co-crystallization of PfTIM–ligand complexes

Conditions that were found suitable for growing well ordered crystals of wild-type PfTIM (hanging-drop setup, 24% PEG 6000 in 100 m*M* HEPES pH 7.5, with 1 m*M* DTT) did not lead to good-quality crystals of PfTIM complexed with the ligands, although the rate of appearance of crystals was generally enhanced. Under these and slightly modified conditions, crystals of complexes were obtained within 3 d. Subsequently, an amorphous deposit on these thin needle-like crystals formed, which made them fragile and unsuitable for high-resolution studies. These crystals belonged to space group $P2_12_12_1$. Replacement of PEG 4000 by PEG 1450 resulted in fewer crystals with larger size and improved morphology. After several trials, the following condition was found to be optimal. The bottom well contained 8–24% of PEG 1450 and 100 m*M* sodium acetate pH 4–5.0. The protein (dialysed against distilled water) concentration was 10 mg ml^{-1}. 3 µl each of protein and the respective ligand in molar ratios of either 1:50 or 1:100 were mixed and allowed to equilibrate for at least 1 h. Crystals appeared within 3–7 d and diffracted to 2.4 Å resolution at room temperature.

2.3. Data collection and processing

Diffraction data from the crystals were collected at room temperature using a MAR300 image-plate system mounted on a Rigaku RU-200 rotating-anode X-ray generator equipped with a 200 µm focal cup. The initial examination of the data frames showed that the crystals of the TIM–3PG and TIM–G3P complexes have similar unit-cell parameters (Table 1) and belong to the monoclinic space group $P2_1$. The asymmetric units correspond to a dimer, with a Matthews coefficient of 2.26 Å^3 Da^{-1} calculated using a molecular weight of 55 662 Da for the TIM dimer. For the TIM–3PG complex, 200 frames were collected, each of 1° oscillation. The crystal-to-detector distance (*D*) was kept at 100 mm and each frame was exposed for 10 min with two passes. For the TIM–G3P complex, 300 frames were collected using two different orientations, with parameters the same as those used for the TIM–3PG crystal. The data sets were processed using the *DENZO*/*SCALEPACK* (Otwinowski & Minor, 1997) suite of programs.

Table 1
Data-collection and refinement statistics for the PfTIM–3PG and PfTIM–G3P complexes.

Values within parentheses correspond to the last resolution shell (2.49–2.40 Å).

	PfTIM–3PG	PfTIM–G3P
Space group	$P2_1$	$P2_1$
Unit-cell parameters (Å, °)	a = 54.26, b = 51.35, c = 90.36, β = 91.38	a = 54.12, b = 51.08, c = 89.55, β = 91.39
Resolution range (Å)	20.0–2.4	20.0–2.4
No. of obervations	73117	98166
No. unique reflections	19146	19337
Overall completeness (%)	97.3 (95.3)	96.5 (96.4)
Multiplicity	3.8 (3.7)	5.1 (4.8)
Average $I/\sigma(I)$	10.5 (3.7)	12.3 (4.1)
R_{sym}† (%)	11.6 (39.9)	11.5 (35.6)
Final R_{free}/R_{cryst}‡ (%)	22.6/18.2	21.9/17.9
No. of atoms (protein/water/ligand)	3914/131/22	3914/140/20
Rm.s.d.s		
Bond length	0.013	0.008
Bond angle	1.782	1.486
Mean real-space *R* factor (*A*/*B*) (%)	4.5/4.1	4.7/4.2
Mean real-space correlation coefficient (*A*/*B*) (%)	95.5/95.9	95.3/95.8
Mean *B* values (*A*/*B*) (Å^2)		
Protein	23.01/21.88	25.07/22.92
Ligand	70.46/71.62	76.49/76.05
Water	29.66	30.79
Overall	23.70	25.54

† $R_{sym} = 100 \times \sum|\langle I\rangle - I|/\sum\langle I\rangle$. ‡ $R_{cryst} = 100 \times \sum|(F_{obs} - F_{calc})|/\sum|F_{obs}|$.

2.4. Structure solution and refinement

Molecular replacement (MR; Rossmann, 1990) was carried out using the *AMoRe* suite of programs (Navaza & Saludian, 1997), using the coordinates of wild-type PfTIM as the starting model (PDB code 1ydv), which was determined earlier at 2.2 Å resolution (Velanker *et al.*, 1997). As expected, MR led to a unique solution. The model was further refined using the 'mlf (maximum likelihood in amplitudes)' option of the *CNS* program suite (Pannu & Read, 1996; Brünger *et al.*, 1998). Data between 20.0 and 2.4 Å resolution were used for the refinement, accepting reflections with amplitudes greater than 0.1σ after setting aside 10% of the data for cross-validation (Brünger, 1992; Kleywegt & Brünger, 1996). Anisotropic *B* scaling, bulk-solvent correction and non-crystallographic restraints (twofold) were employed throughout the refinement. After initial rigid-body and positional refinement, σ_A-weighted $2F_o - F_c$ and $F_o - F_c$ maps (Read, 1986) were calculated and visualized using the interactive model-building programs *FRODO* (Jones, 1978) and *O* (Jones *et al.*, 1991).

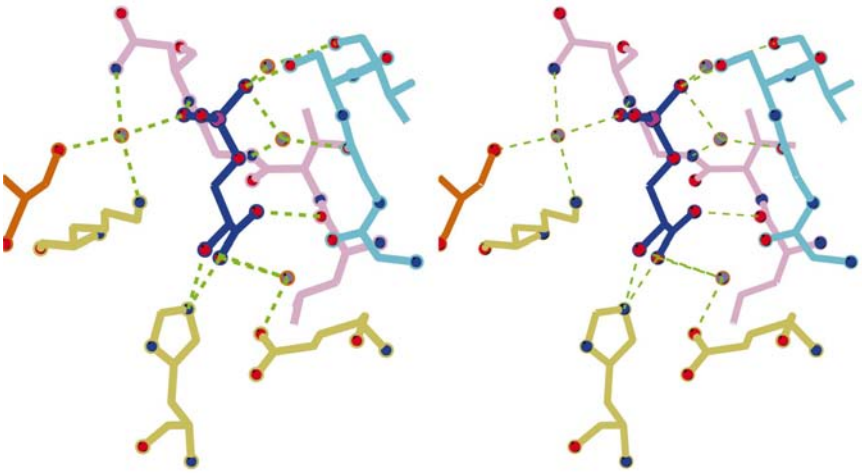

Figure 2
Active-site interactions for the bound 3-phosphoglycerate (3PG) in the *A* subunit of the PfTIM–3PG complex. The ligand and the active-site residues Lys12, His95 and Glu165 are shown in blue and khaki, respectively. Two stretches of residues, Gly209-Gly210-Ser211-Val212 and Leu230-Val231-Gly232-Asn233, anchoring the phosphate group through several water-mediated and direct interactions are shown in cyan and pink, respectively. Ser73, involved in a water-mediated intersubunit interaction in the physiological dimer, is shown in red.

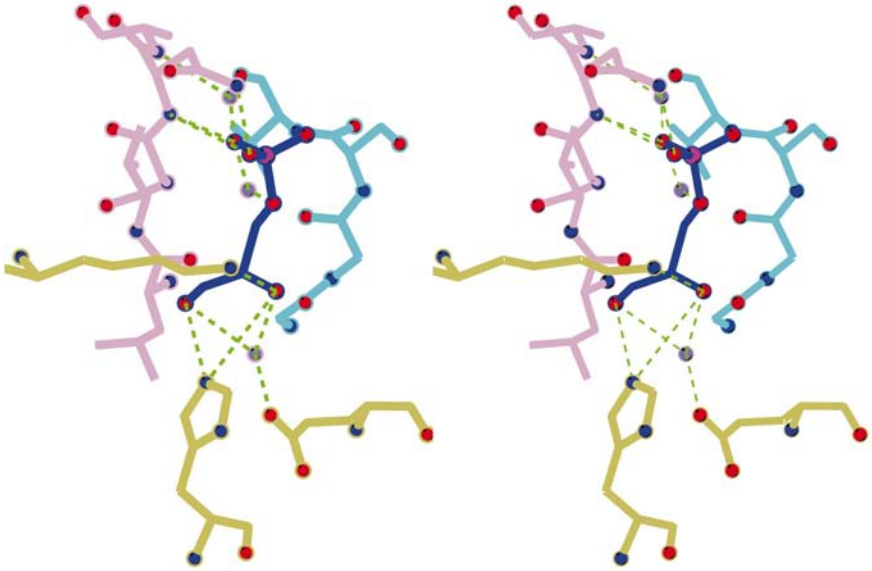

Figure 3
Active-site interactions for glycerol-3-phosphate (G3P) in the *B* subunit of the PfTIM–G3P complex. The ligand and the active-site residues Lys12, His95 and Glu165 are shown in blue and khaki, respectively. Two stretches of residues, Gly209-Gly210-Ser211-Val212 and Leu230-Val231-Gly232-Asn233-Ala234, anchoring the phosphate group through several water-mediated and direct interactions are shown in cyan and pink, respectively.

After building the ligand, a second round of refinement was performed invoking the automatic water-picking algorithm. Positional and *B*-value parameters of all the atoms, including protein, water and ligand atoms, were refined. This was followed by cycles of validation and rebuilding using the programs *OOPS* (Kleywegt & Jones, 1996*a*), *PROCHECK* (Laskowski *et al.*, 1993), *WHAT_IF* (Vriend, 1990) and *O* (Jones *et al.*, 1991). Table 1 lists the relevant refinement statistics. Finally, the coordinates were refined excluding the ligand and surrounding water molecules (15 cycles of position and ten cycles of *B*-value refinement). Omit maps for the ligand and surrounding water molecules were calculated at the end of the refinement.

2.5. Structural analysis

Analyses were performed at three different levels, *viz.* between crystallographically independent subunits, between complexed and uncomplexed PfTIM structures and between PfTIM and TrypTIM structures. Comparisons were made with respect to changes in main-chain and side-chain geometry, changes in active-site residues and changes in the positions of water molecules. Structural alignments were carried out using the programs *ALIGN* (Cohen, 1997) or the lsq_ex option in *O* (Jones *et al.*, 1991). The active-site superpositions were performed using locally available codes. Ligand interactions and symmetry-related contacts were analysed using the programs *LIGPLOT* (Wallace *et al.*, 1995) and *CONTACT* from the *CCP*4 suite (Collaborative Computational Project, Number 4, 1994). Structural illustrations were produced using the programs *MOLSCRIPT* (Kraulis, 1991), *BOBSCRIPT* (Esnouf, 1999), *Raster3D* (Merritt & Bacon, 1997) and *InsightII* (Accelrys, San Diego, CA, USA).

3. Results and discussion

3.1. Structure refinement

Table 1 lists the relevant statistics of data collection and refinement for both PfTIM–3PG and PfTIM–G3P. The completeness of reflection data were 97.3 and 96.5%, with $R_{\rm sym}$ values of 11.6 and 11.5% for PfTIM–3PG and PfTIM–G3P, respectively. The structures were refined to $R_{\rm free}$, $R_{\rm cryst}$ values of 22.6 and 18.2, and of 21.9 and 17.9% for PfTIM–3PG and PfTIM–G3P, respectively (Table 1). The estimated errors based on a Luzzati plot for both the structures were 0.3 Å. The r.m.s. deviation between the two subunits after superposition of C^{α} atoms is 0.25 Å for the PfTIM–3PG complex and 0.24 Å for the PfTIM–G3P complex. The final models have good stereochemistry as shown by the Ramachandran plot (Ramakrishnan & Ramachandran, 1965). Only about 2.6% (12 out of 460) of non-Gly residues have φ, ψ values outside the core region of the Ramachandran plot. (The outliers are defined as residues lying outside the core areas in which 98%

Table 2
Distances between protein and ligand atoms in the PfTIM–3PG complex using a cutoff value of 3.8 Å.

A subunit			*B* subunit		
Ligand atom	Protein atom	Distance (Å)	Ligand atom	Protein atom	Distance (Å)
O1	Wat563W O	3.27	O1	Glu165*B* OE2	3.75
	Asn10*A* ND2	3.25		His95*B* NE2	2.42
	His95*A* NE2	2.63		Asn10*B* ND2	3.69
O2	Wat563W O	3.38		Wat633W O	2.51
	Leu230*A* O	2.89	O2	Asn10*B* ND2	3.67
	Gly232*A* N	3.11		Val231*B* O	3.62
	Wat581W O	3.04		Gly232*B* N	3.13
O3	Glu165*A* OE2	3.79	O3	Gly209*B* O	2.56
	Wat563W O	3.40		Wat633W O	2.73
	Lys12*A* NZ	3.40	O1P	Wat536W O	2.97
	His95*A* NE2	2.72		Gly232*B* N	3.42
O1P	Wat581W O	2.73	P	Wat579W O	3.76
P	Wat581W O	3.38		Asn233*B* N	3.63
O2P	Wat625W O	3.52	O3P	Wat588W O	3.21
O3P	Ser211*A* OG	3.67		Asn233*B* N	3.50
	Wat564W O	2.87		Wat517W O	2.65
	Wat581W O	3.08	O4P	Asn233*B* ND2	2.79
O4P	Lys12*A* NZ	3.80		Wat579W O	2.42
	Wat578W O	2.55		Asn233*B* N	2.77
	Asn233*A* N	3.00			
	Asn233*A* ND2	3.57			

Table 3
Interactions between protein and ligand atoms in the PfTIM–G3P complex using a cutoff value of 3.8 Å.

A subunit			*B* subunit		
Ligand atom	Protein atom	Distance (Å)	Ligand atom	Protein atom	Distance (Å)
O1	Leu230*A* O	3.64	O1	His95*B* NE2	3.38
	Wat523W O	2.81		Wat620W O	3.12
	His95*A* NE2	3.28		Asn10*B* ND2	3.59
	Asn10*A* ND2	3.61		Leu230*B* O	3.53
O2	Wat523W O	3.66	O2	Wat620W O	3.42
	His95*A* NE2	3.79		Lys12*B* NZ	3.09
	Lys12*A* NZ	3.26	O4P	Lys12*B* NZ	3.78
O4P	Lys12*A* NZ	3.64		Wat584W O	3.68
O1P	Lys12*A* NZ	3.48	O1P	Asn233*B* ND2	2.65
	Asn233*A* N	3.37		Asn233B N	3.21
	Wat630W O	3.66	O3P	Asn233*B* N	2.59
	Asn233*A* ND2	3.10		Wat584W O	3.37
O2P	Ser211*A* OG	3.19		Wat517W O	2.33
O3P	Gly232*A* N	3.22		Gly232*B* N	3.04
	Asn233*A* N	2.56	P	Asn233*B* ND2	3.76
P	Wat621W O	3.41		Asn233*B* N	3.45
	Asn233*A* N	3.53		Wat517W O	3.61

of all non-Gly residues were found to lie in a sample of 403 PDB structures with $\leq$95% sequence identity at resolution 2.0 Å or better; Kleywegt & Jones, 1996*b*.) The only non-Gly residue that shows a positive φ is Lys12 (49.5/52.5 and 54.7/50.9° in the *A*/*B* subunits of the 3PG and G3P complexes, respectively). Indeed, this residue has a positive φ in the unbound PfTIM and also in enzymes from other sources (Noble *et al.*, 1991; Alvarez *et al.*, 1998; Zhang *et al.*, 1994). The ligands were well defined in both the crystallographically independent subunits, although the ligands are better defined in one of the subunits than in the other. Fig. 1 shows the electron density for 3PG and G3P in these subunits. The observed break in the electron density for G3P seen in one of the subunits could be a consequence of both partial occupancy and dynamic disorder. The group occupancies for G3P were refined to a values of 0.86 and 0.96 in the *A* and *B* subunits, respectively.

3.2. Protein–ligand interactions

3.2.1. PfTIM–3PG complex. No significant differences in the conformation of the polypeptide fold are observed between the *A* and *B* subunits of the PfTIM–3PG complex. Table 2 gives all polar contacts within 3.8 Å made by the atoms of 3PG in the *A* and *B* subunits. Fig. 2 shows the active-site interactions in the *A* subunit. Water molecules mediate the majority of the contacts between the ligand and the protein atoms (Fig. 2). Indeed, the interaction between the carboxy end of the ligand, which corresponds to the reactive end of the substrate (dihydroxyacetone phosphate, DHAP or D-glyceraldehyde-3-phosphate; D-GAP) and the catalytic base Glu165 is also water-mediated. The almost identical distances between the interacting atoms of the protein and the 3PG O1 and O3 atoms are indeed in agreement with the suggested *cis*-enediol transition state (Alber *et al.*, 1981). The main-chain N atom of Gly232 interacts with O2 of 3PG in both the subunits. At the other end, the phosphate group of 3PG is held by several water-mediated interactions. The catalytic residue Lys12 interacts with one of the O atoms of phosphate group through a water molecule. The only direct interactions between the phosphate group and protein atoms are those involving O3P–Ser211 and O4P–Asn233 in the *A* subunit and O3P and O4P with Asn233 in the *B* subunit.

3.2.2. Catalytic loop (loop 6) conformation. In essentially all TIM–ligand complexes reported so far, the flexible catalytic loop (loop 6, residues 166–176) adopts a closed conformation, with the main-chain NH of Gly171 forming a hydrogen bond with one of the phosphate O atoms of the bound ligands. The transition from the loop-open (unliganded TIM) to the loop-closed (liganded TIM) form involves a large movement (approximately 7.0 Å) of the flexible loop. The only example of a ligand-bound TIM with an open-loop conformation is that of TrypTIM bound to the competitive inhibitor *N*-hydroxy-4-phosphonobutanamide (4PBH; Verlinde *et al.*, 1992).

Interestingly, in the PfTIM–3PG complex, the flexible loop remains in the open conformation. The interaction between 3PG and the main-chain NH of Gly171 is water-mediated in both subunits of the PfTIM–3PG complex. Two and three water molecules seem to bridge this interaction in the *A* and *B* subunits, respectively. In the *B* subunit, water molecule 631 is placed at a distance of 2.39 Å from the main-chain N of Gly171. The distance between this water molecule and the next water molecule (589) is 3.13 Å. Water molecule 589 interacts with 579 at a distance of 3.46 Å and this in turn interacts with O2P of 3PG at a distance of 3.31 Å. Water molecule 579 also interacts with the side chain of Ser73 (from the neighbouring subunit).

In the PfTIM–3PG complex, the absence of a stabilizing interaction involving the loop residue (Gly171) appears to be compensated for by an interaction contributed by the neighbouring subunit. In both the *A* and the *B* subunits, Ser73 is involved in a water-mediated interaction with a phosphate O atom of the ligand bound to the other subunit. The OH group of this residue is at a distance of 2.56 Å from water 578, which in turn is at a distance of 2.55 Å from O4P of the phosphate group of 3PG in the *A* subunit. The corresponding water is 579 in the *B* subunit and the distances involved are 2.46 and 2.42 Å, respectively. The OH group of Ser73 also appears to interact with the side-chain NH_2 groups of Lys12 and Asn233. However, N of Gly171, the flexible-loop residue, interacts with one of the O atoms of the phoshate group *via* one or more water molecules. It is noteworthy that in most of the TIM sequences residue 73 is Ala, whereas in PfTIM there is a Ser at this position.

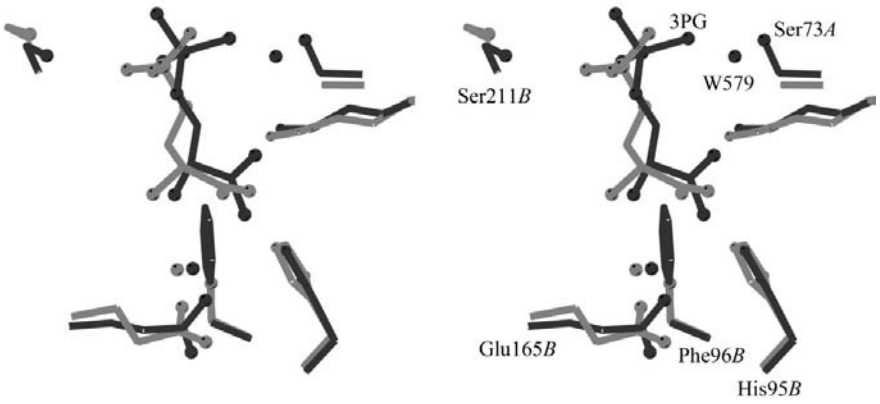

Figure 4
Stereoview of the active-site superposition of the 3PG complex of PfTIM (dark) and TrypTIM (light). Catalytic base Glu165, catalytic acid His95 and electrophile Lys12 are shown along with residues 73 (from a neighbouring subunit), 96 and 211 (PfTIM numbering). Residues Ser73 and Phe96 in PfTIM are Ala and Ser, respectively, in other TIM sequences. Ser213 takes a positive φ value in the TrypTIM–3PG complex.

3.2.3. PfTIM–G3P complex. Inspection of the PfTIM–G3P complex reveals that most of the ligand–protein interactions observed in the 3PG–PfTIM complex are retained in PfTIM–G3P. Table 3 lists all polar contacts within 3.8 Å between the atoms of G3P and the *A* and the *B* subunits of PfTIM. Fig. 3 shows the active-site interactions in the *B* subunit. In contrast to the PfTIM–3PG complex, the ligand is best defined in the *B* subunit in the PfTIM–G3P complex. The interactions between the phosphate moiety and the residue stretches 209–212 and 230–234 in the PfTIM–G3P complex are similar to those found in the PfTIM–3PG complex. At the other end of the ligand, the catalytic base Glu165 interacts with O1 of G3P through a water molecule (523 in the *A* subunit) as observed in the PfTIM–3PG complex. Furthermore, none of the atoms of the catalytic loop are at interacting distances with any of the ligand atoms. The loop has adopted the open conformation and the loop residue Gly171 is involved only in water-mediated interaction with the phosphate of G3P in both the *A* and *B* subunits.

3.3. Comparison of structures of liganded and unliganded PfTIM

3.3.1. PfTIM–3PG complex. After superposition of corresponding C^{α} atoms, the r.m.s. deviation of C^{α} positions between the *B* subunits of unbound PfTIM and PfTIM–3PG and PfTIM–G3P complexes are 0.22 and 0.26 Å, respectively. All the C^{α} atoms superpose well, except for residues 152–155 where the deviations are 1.30, 4.24, 3.03 and 1.76 Å, respectively. These deviations might arise from differences in the crystal packing environments. In the active site of uncomplexed PfTIM, several water molecules are involved in a hydrogen-bonding network with the residues surrounding the active site. Of these, water molecules that interact with residues Glu165, Ser73 (of the neighbouring subunit) and Gly232 are also retained in the active site of both the subunits of the PfTIM–3PG complex. However, two water molecules, near His95 and near Glu97 and Leu230, are either displaced or expelled from the active site on binding of 3PG to the PfTIM *A* subunit. O1 and C2 atoms of the ligand replace two water molecules near His95. 3PG also displaces three other water molecules (590, 650 and 653 of 1ydv) and O atoms of a phosphate group occupy these positions. Similar changes in the position and interaction of water molecules are also seen in the *B* subunit upon ligand binding. No significant changes in the torsion angles of the catalytic residues Glu165, His95 and Lys12 are observed on ligand binding in both the subunits. The only other residue with significant change in side-chain torsion angle χ_2 is Asn233, which contributes a hydrogen bond to the phosphate group of the ligand. The χ_2 values of this residue before and after binding of the ligand are (90, −124°) for the *A* and (7, −65°) for the *B* sununit.

3.3.2. PfTIM–G3P complex. The positions previously occupied by water molecules near His95 are also replaced by O1 and C1 of G3P in both the subunits of PfTIM–G3P. The (χ_1, χ_2) values of Asn233 in the unbound and G3P-bound structures are (−116, 90°) and (−88, −150°), respectively, in the *A* subunit. Similarly, the χ_1 values of Ser211 are −53 and −102° in unbound and G3P-bound PfTIM, respectively. However, there is no significant change in the χ_1 value of Ser211 in the *B* subunit of the PfTIM–G3P complex.

3.4. Comparison of the active site of ligand-bound PfTIM and TrypTIM

3.4.1. Active site. The structures of the 3PG and G3P complexes of TrypTIM are available at comparable resolution (Noble *et al.*, 1991). The active-site superposition of the 3PG complexes of Pf and TrypTIMs reveals that similar interactions from the stretches 208–214 and 232–234 (PfTIM numbering) hold the phosphate end of the ligands in both the Pf and TrypTIM complexes. Fig. 4 shows the superposition of

the active-site residues. As in the PfTIM complexes, the catalytic Glu167 is involved in a water-mediated interaction with the ligand atoms in the G3P and 3PG complexes of TrypTIM. However, the conformations of the side chain of the catalytic base are different in the two enzymes. Noble *et al.* (1991) have described two distinct conformations for Glu167 that differ in the sign of their χ_1 values. A positive χ_1 value of about 55° corresponds to the 'swung-in' conformation where OE2 of Glu points towards the ligand. The negative value defines the 'swung-out' conformation in which OE2 of Glu points away from the ligand. In TrypTIM, swung-in and swung-out conformations were observed for G3P and 3PG complexes, respectively. It was suggested that only the swung-in conformation is suitable for catalysis. However, in PfTIM–3PG and PfTIM–G3P, χ_1 of Glu165 is −55 and −59°, respectively, and OE2 points towards an invariant water molecule which in turn interacts with the ligand. Another notable difference is the contribution of the adjacent subunit to the ligand-binding interaction in PfTIM. The residues Ser73–Tyr74 of PfTIM are Ala73–Phe74 in most other TIM sequences. This natural substitution in PfTIM seems to compensate for the loss of hydrogen bonding from the flexible loop (from Gly171 NH). In both the subunits of PfTIM–3PG complex, the side-chain OH of Ser73 originating from the twofold-related subunit of the physiological TIM dimer interacts through a water molecule with one of the phosphate O atoms. This interaction is also seen in the high-resolution (1.1 Å) structure of 2-phosphoglycerate complexed with the malarial enzyme (unpublished results). Thus, this intersubunit interaction in the ligand-bound forms seems to be an invariant feature of the different inhibitor complexes of PfTIM; presumably, it is a compensating interaction in the open-loop form of the ligand–protein complex.

3.4.2. Conformation of the flexible loop. The most notable feature of the structures of the PfTIM–ligand complexes is that the catalytic loop (loop 6) remains in the open conformation. This is in sharp contrast to the structures of the complexes of the same ligand with TrypTIM, where loop 6 is closed and makes key contacts with the inhibitor (Noble *et al.*, 1991). The most significant interactions between the residues on the flexible loop and the ligands in the TrypTIM complexes are a hydrogen bond between Gly173 NH (TrypTIM numbering) and one of the phosphate O atoms and a hydrophobic interaction involving Ile172. Fig. 5 shows the relative positions of the flexible loops of Pf and TrypTIM after superposition of their corresponding C^{α} atoms. Also shown is the active site of the 3PG-bound TrypTIM. Movement of the TrypTIM loop towards the ligand is clearly seen. The loop sequence between the two enzymes is conserved except for Leu167 in PfTIM, which is Val169 in TrypTIM. The maximum deviation of 7.0 Å is observed for Gly173 (PfTIM numbering). The C^{α} atoms of two residues, Ile172 and Gly173 of TrypTIM, which are involved in van der Waals and hydrogen-bonding interactions with the ligand, are at distances of 3.19 and 5.64 Å, respectively, after superposition.

3.4.3. Implications for inhibitor design. Discussions on the mechanistic features of TIM catalysis have generally implicated loop closure as an important determinant of enzymatic activity (Knowles, 1991). The closure of the loop is believed to be essential for preventing phosphate elimination leading to the formation of the toxic product methylglyoxal (Pompliano *et al.*, 1990). Why does PfTIM appear to favour the loop-open conformation in the ligand-bound states? The presence of Phe96 appears to be a cause, since this residue would come

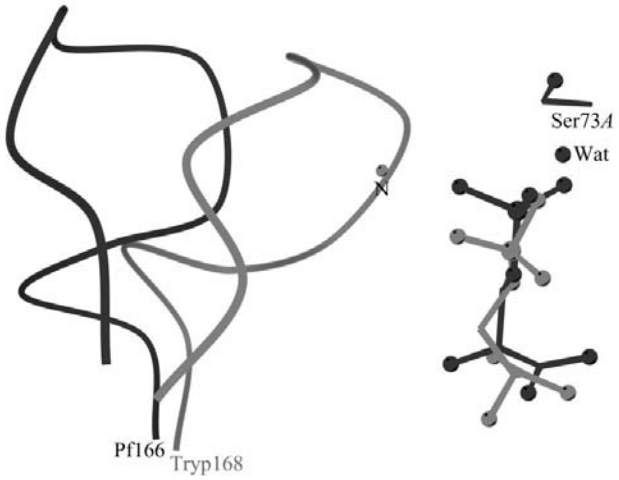

Figure 5
Relative orientation of loop 6 after superposition of C^{α} atoms (*B* subunit) of 3PG complex of Pf (dark) and Tryp (light) TIMs. The main-chain N atom of TrypTIM making a hydrogen bond with 3PG is marked. Water-mediated intersubunit interaction involving Ser73 in PfTIM is also marked (see text for distances).

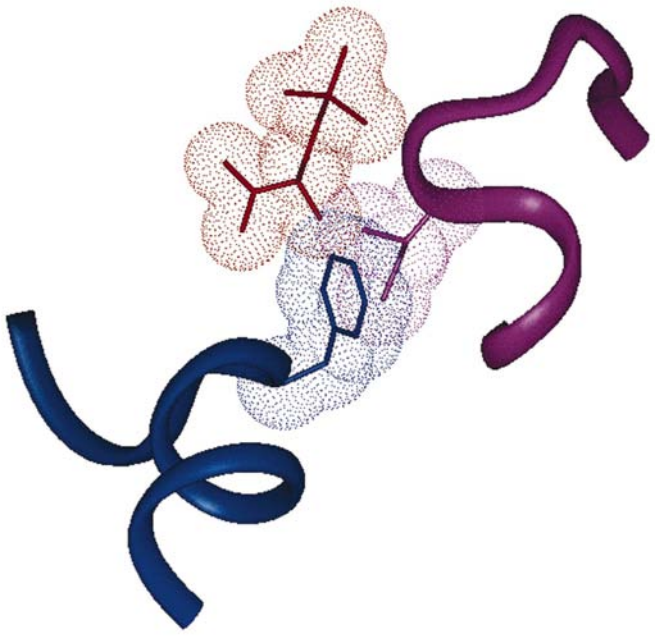

Figure 6
Schematic representation showing the anticipated steric clash between Phe96 and Ile172 of PfTIM in a closed-loop conformation. The figure was generated superposing the PfTIM–3PG structure and the closed-loop TrypTIM structure (PDB code 1iig). van der Waals surfaces for Phe96, Ile (172 in Pf and 174 in TrypTIMs) and 3PG are shown.

into direct steric contact with Ile172 if Phe is modelled into the loop-closed form of TrypTIM. Fig. 6 shows the relative position of the closed loop of TrypTIM–3PG with respect to the active site of PfTIM. Also shown is the active-site helix region of PfTIM containing residue 96, which is Phe in PfTIM and Ser in other TIM sequences. Loop closure leads to severe steric clash between Ile172 and the bulky Phe96 of PfTIM, as can been seen from the overlap of the van der Waals surfaces (Fig. 6) of these residues, presumably destabilizing the closed conformation and making the loop closure less favourable when compared with other TIMs. Clearly, closure of the loop is not important for ligand binding.

The striking structural differences in the enzyme–inhibitor complexes obtained for PfTIM appear to be correlated with the presence of Phe at position 96. Indeed, the Ser96Phe mutation is observed only in the parasite enzyme, while TIMs from all the other species have a conserved Ser at this position. Interestingly, the Ser96Phe mutation is also observed in the sequences of triosephosphate isomerases from *P. berghei*, *P. yeoli*, *P. knowlesi*, *P. chabandi* and *P. vivax*. The PfTIM gene with the Ser96Phe mutation has also been identified in the whole genome sequence of *P. falciparum* (http://www.sanger.ac.uk). This raises the possibility that specific low-molecular-weight inhibitors might be targeted selectively to the active site of the *Plasmodium* enzymes. Inspection of Fig. 6 suggests that the OH group at the C2 atom of 3PG is closest to Phe96 (the distance between O3 of 3PG and CD1 and CE1 atoms of Phe96 are 4.00 and 3.48 Å, respectively). Therefore, it is likely that a suitable substitution at the C2 position of 3PG, which may promote interaction with the aromatic residue, might serve as a lead for the design of parasite-enzyme specific inhibitors. Interestingly, a recent study using a general computer-docking procedure with the coordinates of the unliganded open conformation of PfTIM reveals that several positively charged aromatic dyes might bind at the active site and interact with the unique Phe96 resdiue (Joubert *et al.*, 2001). These dyes are also found to be good inhibitors of the malarial enzyme.

4. Conclusions

Although extensively discussed in the literature (Hermes *et al.*, 1990), there is no consensus on the importance of the conserved residue at position 96 in TIM catalysis (Alber *et al.*, 1987). Structural analysis of a phosphoglycohydroxamate (PGH) complex of chicken TIM Ser96Pro mutant at 1.9 Å resolution revealed altered water structure within the active-site cavity. The activity of the mutant enzyme was 20-fold lower than that of the wild type (Zhang *et al.*, 1999). However, replacement of Ser at position 96 by Phe in the *Plasmodium* enzyme does not impair its catalytic activity (Singh *et al.*, 2001).

NMR studies of yeast TIM suggest a dynamic equilibrium between loop-open and loop-closed forms of the enzyme in solution (Williams & McDermott, 1995). The structures of the two PfTIM–inhibitor complexes described here together with the structure of the PfTIM–phosphoglyclolate (PfTIM–PG) complexes described elsewhere suggest that loop-open conformations are specifically favoured in the case of the parasite enzyme both in the free and ligand-bound states. It is likely that the S96F mutation in the malarial enzyme destabilizes the closed form, permitting trapping of the ligand-bound loop-open states in crystals. The observation of a ligand-bound loop-closed conformation in one of the crystal forms of the PfTIM–PG complex (Parthasarathy *et al.*, personal communication) suggests that loop closure is not completely impeded in the parasite enzyme but is possible if conformational adjustments are made at residues Phe96 and Leu167. These observations are consistent with the observed activity of the parasite enzyme. Further, these structures suggest that selective targeting of the loop-open state by specific inhibitors may be possible, providing an avenue to inhibit the parasite enzyme without affecting the corresponding enzyme in the human host.

The work reported here is supported by grants from the Council of Scientific and Industrial Research (CSIR) and Department of Science and Technology (DST) of the Government of India. The reflection data were collected using the National Facility for Structural Biology supported by the DST and Department of Biotechnology (DBT). Graphics facilities at the Super Computer Education Centre of the institute are acknowledged. SP is the recipient of a CSIR research fellowship.

References

Alber, T. C., Banner, D. W., Bloomer, A. C., Petsko, G. A., Philips, D., Rivers, P. S. & Wilson, I. A. (1981). *Philos. Trans. R. Soc. London Ser. B*, **293**, 159–171.
Alber, T. C., Davenport, R. C. Jr, Giammona, D. A., Lolis, E., Petsko, G. A. & Ringe, D. (1987). *Cold Spring Harbour Symp. Quant. Biol.* **52**, 603–613.
Alvarez, M., Zeelan, J. P., Mainfroid, V., Delrue, F. R., Martial, J. A., Wyns, L., Wierenga, R. K. & Maes, D. (1998). *J. Biol. Chem.* **273**, 2199–2206.
Brünger, A. T. (1992). *Nature (London)*, **355**, 472–475.
Brünger, A. T., Adams, P. D., Clore, G. M., Delano, W. L., Gros, P., Grosse-Kunstleve, R. W., Jiang, J. S., Kuszewski, J., Nilges, M., Pannu, N. S., Read, R. J., Rice, L. M., Simonson, T. & Warren, G. L. (1998). *Acta Cryst.* D**54**, 905–921.
Cohen, G. E. (1997). *J. Appl. Cryst.* **30**, 1160–1161.
Collaborative Computational Poject, Number 4 (1994). *Acta Cryst.* D**50**, 760–763.
Esnouf, R. M. (1999). *Acta Cryst.* D**55**, 938–940.
Hermes, J. D., Blacklow, S. C. & Knowles, J. R. (1990). *Biochemistry*, **29**, 4099–4108.
Jones, T. A. (1978). *J. Appl. Cryst.* **11**, 268–272.
Jones, T. A., Zou, J. Y., Cowan, S. W. & Kjeldgaard, M. (1991). *Acta Cryst.* A**47**, 110–119.
Joubert, F., Neitz, A. W. H. & Louw, A. I. (2001). *Proteins Struct. Funct. Genet.* **45**, 136–143.
Kleywegt, G. J. & Brünger, A. T. (1996). *Structure*, **4**, 897–904.
Kleywegt, G. J. & Jones, T. A. (1996*a*) *Acta Cryst.* D**52**, 829–832.
Kleywegt, G. J. & Jones, T. A. (1996*b*). *Structure*, **4**, 1395–1400.
Knowles, J. R. (1991). *Nature (London)*, **350**, 121–124.
Kraulis, P. J. (1991). *J. Appl. Cryst.* **24**, 946–950.
Laskowski, R. A., MacArthur, M. W., Moss, D. S. & Thornton, J. M. (1993). *J. Appl. Cryst.* **26**, 283–291.

Merritt, E. A. & Bacon, D. J. (1997). *Methods Enzymol.* **277**, 505–524.
Navaza, J. & Saludian, P. (1997). *Methods Enzymol.* **276**, 581–593.
Noble, M. E. M., Wierenga, R. K., Lambeir, A. M., Opperdoes, F. R., Thunnissen, A. M. W. H., Kalk, K. H., Groendijk, H. & Hol, W. G. J. (1991). *Proteins Struct. Funct. Genet.* **10**, 50–69.
Olliaro, P. L. & Yuthavong, Y. (1999). *Pharmacol. Ther.* **81**, 91–110.
Otwinowski, Z. & Minor, W. (1997). *Methods Enzymol.* **276**, 307–325.
Pannu, N. S. & Read, R. J. (1996). *Acta Cryst.* A**52**, 659–668.
Pompliano, D. L., Peyman, A. & Knowles, J. R. (1990). *Biochemistry*, **29**, 3186–3194.
Ramakrishnan, C. & Ramachandran, G. N. (1965). *Biophys. J.* **5**, 909–933.
Ranie, J., Kumar, V. P. & Balaram, H. (1993). *Mol. Biochem. Parasitol.* **61**, 159–170.
Read, R. J. (1986). *Acta Cryst.* A**42**, 140–149.
Rossmann, M. G. (1990). *Acta Cryst.* A**46**, 73–82.
Roth, E. Jr, Kuvlin, V., Miwa, S., Yoshida, A., Akatusuka, J., Cohen, S. & Rosa, R. (1988). *Blood*, **71**, 1408–1413.
Singh, S. K., Kapil, M, Balaram, H. & Balaram, P. (2001). *FEBS Lett.* **501**, 19–23.
Subbayya, I. N. S., Ray, S. S., Balaram, P. & Balaram, H. (1997). *Ind. J. Med. Res.* **106**, 79–94.
Velanker, S. S., Ray, S. S., Gokhale, R. S., Suma, S., Balaram, H., Balaram, P. & Murthy, M. R. N. (1997). *Structure*, **5**, 751–761.
Verlinde, C. L. M. J., Witmans, C. J., Pijning, T., Kalk, K. H., Hol, W. G. J., Callens, M. & Opperdoes, F. R. (1992). *Protein Sci.* **1**, 1578–1584.
Vriend, G. (1990). *J. Mol. Graph.* **8**, 52–56.
Wallace, A. C., Laskowski, R. A. & Thornton, J. M. (1995). *Protein Eng.* **8**, 127–134.
Williams, J. C. & McDermott, A. E (1995). *Biochemistry*, **34**, 8309–8319.
Winstanley, P. A. (2000). *Parasitol. Today*, **16**, 146–153.
Zhang, Z., Komives, E. A., Suigio, S., Blacklow, S. C., Narayana, N., Xuong, H. N., Stock, A. M., Petsko, G. A. & Ringe, D. (1999). *Biochemistry*, **34**, 4389–4397.
Zhang, Z., Sugio, S., Komives, E. A., Liu, K. D., Knowles, J. R., Petsko, G. A. & Ringe, D. (1994). *Biochemistry*, **33**, 2830–2837.